

Heart Rate Reduction With Ivabradine Protects Against Left Ventricular Remodeling by Attenuating Infarct Expansion and Preserving Remote-Zone Contractile Function and Synchrony in a Mouse Model of Reperfused Myocardial Infarction

Daniel M. O'Connor, BA; Robert S. Smith, MD; Bryan A. Piras, PhD; Ronald J. Beyers, PhD; Dan Lin, PhD; John A. Hossack, PhD; Brent A. French, PhD

Background—Ivabradine selectively inhibits the pacemaker current of the sinoatrial node, slowing heart rate. Few studies have examined the effects of ivabradine on the mechanical properties of the heart after reperfused myocardial infarction (MI). Advances in ultrasound speckle-tracking allow strain analyses to be performed in small-animal models, enabling the assessment of regional mechanical function.

Methods and Results—After 1 hour of coronary occlusion followed by reperfusion, mice received 10 mg/kg per day of ivabradine dissolved in drinking water ($n=10$), or were treated as infarcted controls ($n=9$). Three-dimensional high-frequency echocardiography was performed at baseline and at days 2, 7, 14, and 28 post-MI. Speckle-tracking software was used to calculate intramural longitudinal myocardial strain (E_{ll}) and strain rate. Standard deviation time to peak radial strain ($SD T_{peak} E_{rr}$) and temporal uniformity of strain were calculated from short-axis cines acquired in the left ventricular remote zone. Ivabradine reduced heart rate by 8% to 16% over the course of 28 days compared to controls ($P<0.001$). On day 28 post-MI, the ivabradine group was found to have significantly smaller end-systolic volumes, greater ejection fraction, reduced wall thinning, and greater peak E_{ll} and E_{ll} rate in the remote zone, as well as globally. Temporal uniformity of strain and $SD T_{peak} E_{rr}$ were significantly smaller in the ivabradine-treated group by day 28 ($P<0.05$).

Conclusions—High-frequency ultrasound speckle-tracking demonstrated decreased left ventricular remodeling and dyssynchrony, as well as improved mechanical performance in remote myocardium after heart rate reduction with ivabradine. (*J Am Heart Assoc.* 2016;5:e002989 doi: 10.1161/JAHA.115.002989)

Key Words: dyssynchrony • heart rate • ivabradine • left ventricular remodeling • speckle-tracking echocardiography • strain rate imaging

The newly US Food and Drug Administration–approved heart medication ivabradine selectively inhibits the hyperpolarization-activated cyclic nucleotide-gated (HCN) channels of the sinoatrial node. This blockade results in a reduction of the cardiac pacemaker, or funny, current (I_f),

reducing the slope of the slow diastolic depolarization phase of the sinoatrial node action potential, and thus slowing heart rate.¹ The action of ivabradine on the HCN channel is use dependent, making the drug more potent in patients with elevated heart rate.²

Two large multicenter studies have demonstrated the benefits of ivabradine as a supplement to guideline-based treatment, such as β -blockers and angiotensin-converting enzyme inhibitors, in patients with left ventricular (LV) dysfunction and with heart rates greater than 70 bpm. The BEAUTIFUL trial demonstrated reduced hospital admission for myocardial infarction (MI) and reduced need for coronary revascularization after ivabradine administration to patients with chronic coronary artery disease with LV dysfunction.³ The SHIFT study demonstrated ivabradine's ability to lower the risk of death and hospitalization associated with heart failure.⁴ In the echocardiographic arms of both the BEAUTIFUL and SHIFT trials, treatment with ivabradine was

From the Departments of Biomedical Engineering (D.M.O., R.S.S., B.A.P., R.J.B., D.L., J.A.H., B.A.F.), Surgery (R.S.S.), Radiology (B.A.F.), and Medicine (B.A.F.), University of Virginia, Charlottesville, VA.

Correspondence to: Brent A. French, PhD, Department of Biomedical Engineering, University of Virginia, Box 800759, Charlottesville, VA 22903. E-mail: bf4g@virginia.edu

Received December 15, 2015; accepted March 28, 2016.

© 2016 The Authors. Published on behalf of the American Heart Association, Inc., by Wiley Blackwell. This is an open access article under the terms of the Creative Commons Attribution-NonCommercial-NoDerivs License, which permits use and distribution in any medium, provided the original work is properly cited, the use is non-commercial and no modifications or adaptations are made.

associated with a significant decrease in the LV end-systolic volume index and improved ejection fraction.^{5,6} Subsequently, ivabradine was added to the 2012 European Society of Cardiology guidelines on heart failure, indicated in addition to β -blockers in patients with chronic symptomatic systolic heart failure with heart rates greater than 70 bpm.⁷ Recently, data from the DIAMOND study suggested that the prognostic importance of resting heart rate, independent of concurrent β -blockade, is stronger in patients directly after acute MI compared to patients with heart failure, especially in the short term, suggesting a therapeutic potential of ivabradine in this setting.⁸

We hypothesized that reducing heart rate in the subacute period after MI, prior to the formation of mature scar would reduce cumulative wall stress, which could potentially ameliorate several deleterious biomechanical mechanisms that contribute to LV remodeling.^{9,10} These mechanisms include the following: (1) infarct expansion into the adjacent noninfarcted region; (2) hypertrophy and dilation of noninfarcted myocardium, causing decreased contractile function in the remote zone; and (3) remote zone dyssynchrony.^{9,11} Recent advances in ultrasound imaging techniques, including speckle-tracking at improved spatial and temporal resolutions, enable the serial assessment of end points relevant to these biomechanical properties, even in small-animal models.^{11,12}

Ivabradine has been shown to reduce morbidity and mortality in patients with chronic coronary artery disease and heart failure, and a limited number of preclinical studies have examined the effect of the drug on LV remodeling after acute MI using rat and rabbit permanent ligation models.^{13–17} Recently, data from the VIVIFY trial showed ivabradine to be safe and effective in lowering heart rate after reperfused infarction.¹⁸ Furthermore, a recent paired-cohort pilot study by Gerbaud and colleagues suggested that the addition of ivabradine to current guideline-based therapy may improve LV remodeling when delivered after reperfusion.¹⁹

In this study, we demonstrate the beneficial effects of ivabradine on LV remodeling for the first time in a reperfused mouse model of MI, simulating the predominant clinical situation in which the occluded coronary arteries are recanalized or bypassed. Furthermore, we use recent advances in echocardiographic imaging techniques, integrated with a novel surgical technique to improve image quality, to probe regional mechanical function in the heart post-MI, and demonstrate for the first time that heart rate reduction using ivabradine reduces infarct expansion and preserves remote zone contractile function. Finally, this is also the first study to demonstrate that ivabradine administration attenuates the development of LV dyssynchrony after reperfused MI.

Methods

The experimental design of this study is summarized in Figure 1.

Model of Reperfused MI

Animal protocols used in this study were approved by the Institutional Animal Care and Use Committee at the University of Virginia and conformed to the Guide for the Care and Use of Laboratory Animals (National Institutes of Health publication 85-23, revised 1985). Male C57Bl/6 mice were purchased from Jackson Laboratories (Bar Harbor, ME). They were between 10 and 12 weeks old and weighed 24 to 29 g at the time of surgery. The mice were anesthetized with pentobarbital (50 mg/kg, IP) and the depth of anesthesia was monitored by foot-pinch reflex. A heat lamp and heating pad that received feedback via a rectal thermometer probe were used to maintain a body temperature of $37 \pm 0.5^\circ\text{C}$ throughout the procedure and recovery. PE-60 tubing was used as an endotracheal tube, connected to a respirator (SAR-830/P, Life Science Instruments, CA) set at 100 breaths/min. ECGs

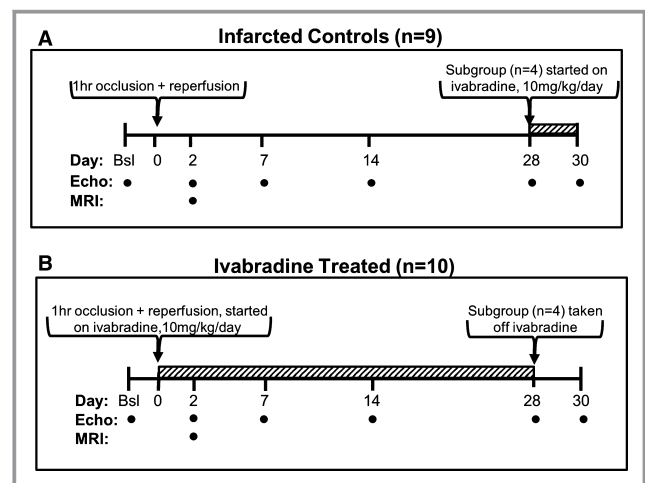


Figure 1. Experimental design. A, Infarcted control mice ($n=9$) received a 1-hour occlusion of the left coronary artery followed by reperfusion. These mice were imaged using echocardiography at baseline and at 2, 7, 14, and 28 days post-MI. MRI was performed on day 2 post-MI in a subgroup of these mice ($n=6$) in order to determine infarct size. On day 28, a subgroup of control animals ($n=4$) was placed on 10 mg/kg per day of ivabradine and imaged on day 30. B, The ivabradine-treated group ($n=10$) underwent left coronary artery occlusion and received 10 mg/kg per day of ivabradine in their drinking water after reperfusion. MRI was performed on day 2 post-MI in a subgroup of these mice ($n=5$) in order to determine infarct size. A subgroup from the ivabradine-treated group ($n=4$) was taken off ivabradine on day 28 and imaged by ultrasound on day 30. bsl indicates baseline; MI, myocardial infarction; MRI, magnetic resonance imaging.

were recorded by a PowerLab module with PowerLab software (ADI Instruments, Colorado Springs, CO).

In order to reduce scarring and improve echocardiographic image quality after MI, we developed a surgical technique that utilizes a small (1–2 cm) transverse incision in the left anterolateral third intercostal space rather than a larger fourth or fifth intercostal space thoracotomy or sternotomy. This was followed by a dissection of the left chest muscles to expose the third and fourth ribs, which, along with the adjacent intercostal muscles, were cut with a cautery pen to expose the chest cavity. The location of this incision is remote from the parasternal echocardiogram window required for short-axis cardiac imaging. A portion of the pericardial sac was removed, and a 7–0 silk suture with a tapered needle was passed under the left coronary artery and was tightened over a length of PE-20 tubing, occluding the artery. Full occlusion was confirmed by a blanching of the myocardium and a widening of the QRS complex. The chest wall was then closed, temporarily. The left coronary artery was left occluded for 1 hour, thus inducing a reproducible transmural infarction in the apex and anterolateral walls of the LV.

After 1 hour, the left coronary artery ligature was removed, allowing for reperfusion. The chest was then closed in 2 layers. The lungs were fully inflated just prior to final closure to prevent pneumothorax. The endotracheal tube was removed when spontaneous breathing occurred, and 100% oxygen administration was continued via a nose cone until the animal awoke. Ketoprofen was administered as needed for pain management.

Ivabradine Administration

After reperfusion, mice were randomly divided into treatment (n=10) and control (n=9) groups. The treatment group received 10 mg/kg per day of ivabradine, a dose similar to previous animal studies.^{14–17,20} This dose was previously shown to be the highest dose that can effectively be administered to mice via drinking water.²⁰ The drug was dissolved in the animals' drinking water, using a concentration based on pilot studies measuring the average amount of water consumed per day (data not shown). The control group received normal water. Ivabradine administration was not found to affect daily water consumption. On day 28 post-MI, a subgroup in the ivabradine-treated group (n=4) was taken off the drug. In addition, a subgroup from the control group (n=4) was switched to 10 mg/kg per day of ivabradine.

Magnetic Resonance Imaging

Infarct sizes were determined in a randomly selected subgroup of animals on day 2 post-MI using late gadolinium-enhanced cardiac magnetic resonance imaging (MRI; n=5

ivabradine-treated, n=6 infarcted controls), as described previously.²¹ MRI scanning was conducted 12 to 14 hours prior to day 2 echocardiography in order to ensure the mice had adequate time to recover between scanning sessions. Anesthesia was induced using a 3% mixture of isoflurane gas and oxygen, delivered via nose cone, which was maintained at 1% during imaging. Pediatric ECG leads (Blue Sensor, BRS-50-K/US; Ambu, Linthicum, MD) were attached to the shaved limbs of the mice for cardiac gating, and a pneumatic respiration sensor was placed just inferior to the diaphragm for respiratory gating of the MRI scanner. ECG, respiration, and body temperature were monitored during imaging using an MRI-compatible system (SA Instruments, Stony Brook, NY). Body temperature was maintained at $37.0\pm 0.5^{\circ}\text{C}$ by circulating temperature-controlled warm water under the mice. A length of PE-20 tubing was surgically inserted into the peritoneal cavity for the intraperitoneal infusion of gadolinium diethylenetriamine pentaacetic acid (0.1–0.2 mmol/kg) contrast agent.

A small-bore 7-T scanner (ClinScan, Bruker, Ettlingen, Germany) was equipped with a radiofrequency 4-channel body coil for mice and gradient system capable of 650 mT/m maximum strength and 6667 mT/(m·ms) maximum slew rate. Localizer imaging was performed to identify double-oblique long-axis (LA) and short-axis (SA) views of the LV, followed by multislice inversion-recovery imaging, 10–15 minutes after gadolinium diethylenetriamine pentaacetic acid infusion.

Echocardiography

Mice were studied by echocardiography at baseline and at 2, 7, 14, and 28 days post-MI using a Vevo 2100 micro-imaging system with a MS400 30-MHz linear array transducer. In order to achieve the highest possible image quality, mice were excluded from the trial before surgery if baseline scans displayed artifacts or poor visualization of the epicardial and endocardial borders caused by anatomical variations. Prior to scanning, fur was removed from the chest area using an electric shaver followed by depilation with potassium thioglycolate cream (Nair, Church & Dwight Co., Princeton, NJ).

Ultrasound B-mode cardiac image sequences were acquired using a Vevo 2100 high-resolution ultrasound scanner (VisualSonics Inc., Toronto, Ontario, Canada). During scanning, the mice were maintained under light anesthesia using an inhaled mixture of 1.4% isoflurane gas and atmospheric air. Mice were placed supine on a platform with an electrical heating unit and core body temperature was monitored with a rectal temperature probe and maintained at $37.0\pm 0.2^{\circ}\text{C}$ to minimize heart rate variation. ECG signals were obtained by coating mouse limbs with electrically conductive gel and taping them to ECG electrodes integrated into the platform. Heart rates were recorded at 20 to 25 time

points over the course of each echocardiographic imaging session.

A custom hardware/software interface was developed to control the motor stage holding the ultrasound transducer and trigger the scanner to acquire and store data, which allowed for the automatic acquisition of finely sampled 2-dimensional short-axis cines, providing for a 3-dimensional assessment of the left ventricle. Ten to 14 serial parasternal LV short-axis cines were captured from the apex to the base of the LV at 0.5-mm intervals. Care was taken to maximize endocardial and epicardial border visibility and to minimize artifacts. Three cardiac cycles were captured per SA view, with an average of 30 to 40 frames per cardiac cycle (≈ 330 – 400 frames per second). The transducer probe was then rotated 90 degrees to obtain a vertical LA image (bisecting the mitral valve and intersecting the LV apex), with an average of 25 to 35 frames recorded per cycle (≈ 260 – 300 frames per second). The total ultrasound imaging session duration was ≈ 30 minutes per mouse, with ≈ 2 minutes spent on image acquisition per mouse, capturing the full SA sweep from apex to base and vertical LA cine.

Volumetric Analysis

LV SA cross-sectional areas and LA length (from mitral annulus to the apex) were calculated using the Vevo 2100 scanner's cardiac measurement package. Endocardial contours were manually delineated at end-diastole and end-systole at 0.5-mm intervals from apex to base using 2 to 3 cardiac cycles per SA interval. The LV end-systolic volumes (ESV) and LV end-diastolic volumes (EDV) were then computed using a modified Simpson's summation of disks. Ejection fraction (EF) and stroke volume were derived from these volumes. A single, trained operator (D.M.O.) performed all tracings and analysis.

The extent of wall thinning was calculated from endocardial and epicardial traces of LA images at end-diastole. Significant wall thinning was defined as LV wall thickness of 0.5 mm or thinner, relative to the normal end-diastolic wall thickness of approximately 1 mm. The extent was defined as the percentage of the LV wall in which significant wall thinning occurred.²²

Strain Analysis

Intramural longitudinal myocardial strain (E_{ll}) and strain rate were computed over the course of the cardiac cycle for each animal at baseline and on days 2, 7, 14, and 28 post-MI. Longitudinal strain was chosen for strain analysis because it has been shown to be more sensitive and reliable than circumferential and radial strain for measuring LV function and has been demonstrated to have strong clinical relevance.^{23–25}

Analyses were conducted on all animals by the same trained investigator (D.M.O.) using the VisualSonics VevoStrain speckle-tracking software package. Suitable cardiac cycles were selected from LA B-mode cines of multiple cycles based on the ability to visualize the endocardial and epicardial borders, absence of respiratory motion, and fewest number of image artifacts. The endocardial and epicardial borders were traced at end-diastole, and the speckle-tracking algorithm tracked the contours over the course of the cardiac cycle. The initial traces were corrected, as needed, to assure faithful tracking throughout the complete cardiac cycle. Each vertical LA view of the LV myocardium was divided into 6 standard anatomic segments for regional speckle-tracking.^{26,27} The mid-anterior, apical-anterior, and apical-inferior wall segments were designated as the infarct region and the basal-inferior and mid-inferior wall segments were designated as the remote zone.²³

Dyssynchrony Analysis

In order to assess contractile dyssynchrony in the LV, regional time to peak radial strain ($T_{\text{peak } E_{rr}}$) was measured from SA slices taken 1.5 to 2 mm from the base of the LV. This location was chosen because it is largely spared from infarction, and the intent of dyssynchrony analysis was to interrogate noninfarcted regions that might retain the capacity for synchronous contraction. Radial strain was chosen for the assessment of dyssynchrony rather than longitudinal strain, which was used for assessment of LV contractile function, given that radial strain has been shown to be more sensitive and clinically relevant in dyssynchrony analysis, particularly for identifying potential responders to cardiac resynchronization therapy.^{28–30}

The standard deviation of the regional $T_{\text{peak } E_{rr}}$ ($SD T_{\text{peak } E_{rr}}$) is a measure of the disparity in timing of regional myocardial motion, and was used as a cardiac dyssynchrony index. Cardiac dyssynchrony was also quantified using the temporal uniformity of strain (TUS).^{29,31} This metric is computed by subjecting the radial displacements of 48 sectors around the SA circumference at the end-systolic phase to Fourier decomposition. TUS is then computed using the following formula:

$$TUS = \sqrt{\frac{A_0^2}{A_0^2 + 2A_1^2}}$$

where A_0 and A_1 are the zero- and first-order Fourier transform terms.²⁹ Thus, TUS is a ratio of the synchronous (uniform) component of radial displacement to the sum of the synchronous and dyssynchronous components of radial displacement. A TUS of 1 indicates synchronous contraction, while a TUS value decreasing toward 0 indicates increasingly dyssynchronous contraction.

Statistical Analysis

Continuous data are presented as mean±SE. The Shapiro–Wilk test was used to assess the normality of the data. Two-factor mixed ANOVA was used for all analyses involving the interaction of treatment group and time, with post-hoc analyses (Tukey's tests) performed where appropriate. Groups from the day 30 post-MI crossover study were compared using Kruskal–Wallis 1-way ANOVA and post-hoc analysis was performed using Dunn's multiple-comparison test with a Bonferroni adjustment for multiple comparisons. All other comparisons were performed using the Mann–Whitney *U* test or Student's *t*-test where appropriate. $P<0.05$ was considered significant in all comparisons. Analyses were performed using STATA version 13.1 (StataCorp LP, College Station, TX).

Results

Mouse Mortality

Of the 45 mice scanned at baseline, 32 were considered to have high-quality baseline scans (clearly visible epicardial and endocardial contours and minimal imaging artifacts) and underwent infarct surgery. Mortality rate during surgery was 38%. One mouse in the control group died on day 3 post-MI, and the remaining 9 infarcted control and 10 ivabradine-treated mice completed the study. None of the surviving mice needed to be excluded from any part of the subsequent analysis based on image quality.

Ivabradine Administration Attenuates Post-MI LV Remodeling

LV EDV and ESVs were measured by echocardiography from 8 to 12 SA slices and 1 vertical LA slice (Figure 2A), 1 to 3 days before surgery (baseline) and on days 2, 7, 14, and 28 post-MI. Late gadolinium-enhanced MRI performed on day 2 in a subset of mice ($n=6$ infarcted controls and $n=5$ ivabradine-treated) confirmed no significant difference in acute infarct size as a percent of LV mass between groups (controls= $31.4\pm 1.1\%$ of LV mass, ivabradine-treated= $30.0\pm 2.3\%$ of LV mass; $P=0.65$). Heart rates, as sampled through the course of echocardiography scanning sessions, increased from 505 ± 11 and 509 ± 11 bpm at baseline in the control and ivabradine groups, respectively, to 598 ± 15 and 549 ± 14 bpm, on day 2 post-MI (Figure 2B). As remodeling progressed, ivabradine administration was found to result in a significant reduction in heart rate at all time points post-MI, from an 8.5% reduction on day 2 ($P<0.05$) to 16.3% on day 28 post-MI ($P<0.0005$) compared to the infarcted controls at the same time points. On day 28 post-MI, heart rates were 627 ± 9 and 533 ± 14 bpm in the control and ivabradine-treated groups, respectively.

ESV (Figure 2C) and EDV (Figure 2D) increased progressively in both control and ivabradine-treated groups, with no significant differences between the groups at days 2 or 7 post-MI. In the control group, EDV and ESV continued to increase until day 28 (2.1 ± 0.2 - and 5.8 ± 0.8 -fold over baseline, respectively). By contrast, the ivabradine-treated group showed no significant increases in EDV or ESV after day 7 post-MI. The ivabradine group showed a 32% reduction in ESV compared to the control group at day 14 ($P<0.05$), and a 36% reduction in ESV at day 28 (60.3 ± 6.0 μL for ivabradine versus 86.5 ± 8.5 μL for controls on day 28; $P<0.05$). EDV in the ivabradine group was 12% lower than the control group at day 14 ($P=0.16$) and reached a statistically significant difference on day 28 post-MI (109.1 ± 7.3 μL for ivabradine versus 130.0 ± 9.0 μL for controls on day 28; $P<0.05$). The ivabradine-treated group had a significantly greater EF from day 14 onward, and by day 28, EF was $33.5\pm 2.7\%$ for control mice and $45.4\pm 2.5\%$ for the ivabradine group (Figure 2E, $P<0.01$).

Acute and Chronic Effects of Ivabradine Administration After MI

In order to examine the difference between the effects of chronic ivabradine administration over the course of remodeling and the acute effects of ivabradine administration, a crossover study was performed. A subgroup of 4 control mice was placed on ivabradine, and a subgroup of 4 mice from the ivabradine group was taken off the drug on day 28 post-MI, by which time the majority of LV remodeling is complete in mice.³² Echocardiography was performed on both subgroups on day 30. Animals from the ivabradine group whose treatment was halted maintained 12% lower heart rates (Figure 3A) and a 27% improvement in EF (Figure 3C) compared to mice that were never treated with the drug ($P<0.001$ and <0.05 , respectively). Mice treated with ivabradine for 28 days showed a 31% smaller ESV ($P<0.05$, Figure 3B) as well as 23% greater EF than acutely treated control mice ($P<0.05$). Mice acutely treated with ivabradine showed a 10% decrease in heart rate compared with control animals (Figure 3A; $P<0.01$). These mice also showed a 9% improvement in EF, although this trend did not reach statistical significance.

Ivabradine Administration Reduces the Extent of Wall Thinning After MI

Representative day 28 post-MI LA echo images of control and ivabradine-treated mouse hearts at end-diastole are shown in Figure 4A and 4B, illustrating the reduced extent of wall thinning in the ivabradine-treated group. Figure 4C demonstrates that the extent of wall thinning, measured as

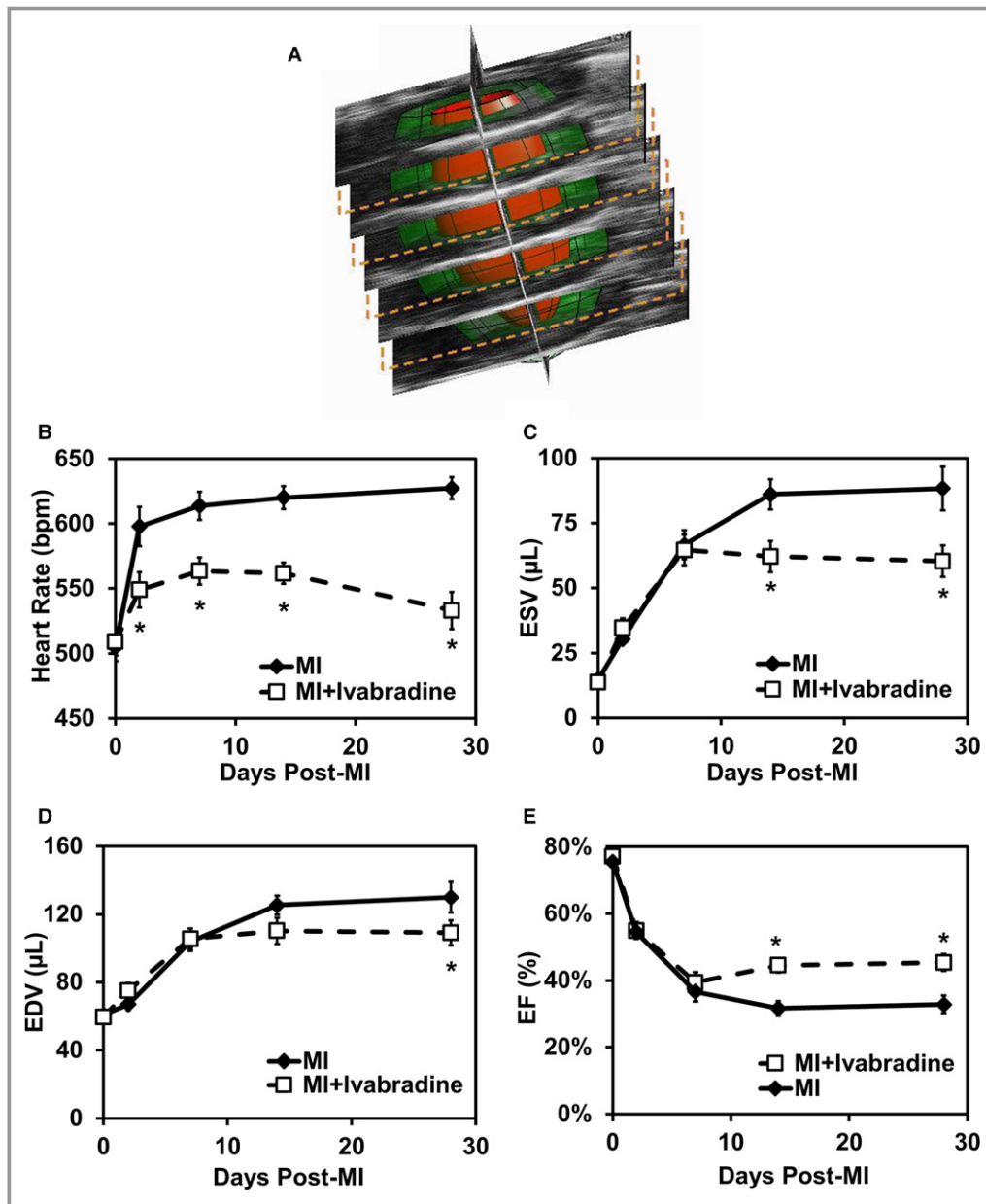


Figure 2. Ivabradine administration attenuates post-MI LV remodeling. A, Three-dimensional left ventricular (LV) chamber volumes were calculated by combining a stack of 10 to 12 short-axis and 1 long-axis image. B, Administration of ivabradine reduced heart rate by 8% to 16% over the course of 28 days compared to the infarcted controls. C, LV end-systolic volume (ESV) was significantly reduced in the ivabradine group compared to controls on days 14 and 28. D, LV end-diastolic volume (EDV) was reduced in the ivabradine group, compared to the controls at each time point measured, reaching significance at day 28. E, Ejection fraction (EF) in the ivabradine-treated group was significantly improved over the control group at days 14 and 28 post-MI. * $P < 0.05$ vs infarcted control group at the same time point. Data points in (B through E) represent mean \pm SEM of $n = 9$ infarcted control mice and $n = 10$ infarcted ivabradine mice. MI indicates myocardial infarction; MRI, magnetic resonance imaging.

the percentage of LA tissue with a thickness of less than 0.5 mm at end-diastole, rapidly progressed after MI through day 7, and showed moderate progression from days 7 through 28 in both groups. Of note, the majority of this wall thinning occurred in the infarcted region in the anterior wall.

The extent of wall thinning was reduced by 25% in ivabradine-treated mice compared to infarcted controls as early as day 7 post-MI and remained 21% smaller by day 28 ($34 \pm 2\%$ of LV circumference for ivabradine versus $43 \pm 3\%$ for controls on day 28; $P < 0.05$).

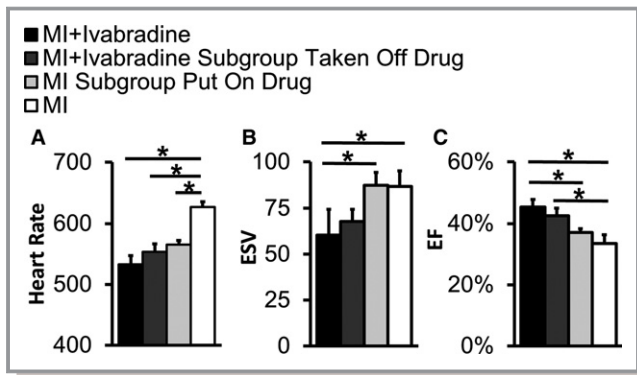


Figure 3. Acute and chronic effects of ivabradine administration after MI. In order to examine the difference between the chronic administration of ivabradine over the course of 28 days and the acute effects of ivabradine after 28 days of LV remodeling, a crossover study was performed. A subgroup of 4 infarcted control mice was placed on ivabradine, and a subgroup of 4 mice from the ivabradine group was taken off the drug on day 28 post-MI. Echocardiography was performed on both subgroups on day 30. A, Animals from the ivabradine group whose treatment was halted maintained 12% lower heart rates compared to mice that were never treated with the drug. Mice acutely treated with ivabradine showed a 10% decrease in heart rate compared with control animals. B, Mice that were treated with ivabradine for 28 days showed 31% smaller end-systolic volumes (ESV) compared with mice acutely administered the drug after 28 days of LV remodeling. C, Animals from the ivabradine group whose treatment was halted showed a 27% improvement in ejection fraction (EF) compared to mice never treated with the drug. These mice also showed 23% greater EF than mice acutely administered ivabradine on days 28 to 30. * $P < 0.05$ for all comparisons. EF indicates ejection fraction; ESV, end-systolic volume; LV, left ventricular; MI, myocardial infarction.

Ivabradine Administration Improves Longitudinal Strain and Strain Rate in Noninfarcted Myocardium

Speckle-tracking analysis of long-axis images was performed at baseline and days 2, 7, 14, and 28 after MI to determine the effects of ivabradine on regional and global peak longitudinal strain ($E_{||}$) and strain rate. Baseline strain and strain rate values were in good agreement with previously published values using the same scanner model and analysis software.²³ Global analyses revealed $E_{||}$ reductions from baseline to day 2 post-MI of -17.8 ± 0.5 to -11.8 ± 0.6 in controls and -18.6 ± 0.7 to -11.6 ± 1.1 in the ivabradine group (34% and 37% reductions in the control and ivabradine groups, respectively; Figure 5A). While peak strain continued to decline in the control group, it leveled off after day 2 in the ivabradine-treated group, leading to significant differences between the two groups on days 14 and 28. $E_{||}$ was 44% higher in the ivabradine-treated group compared to the controls on day 28 post-MI (-11.8 and -8.2 in the ivabradine

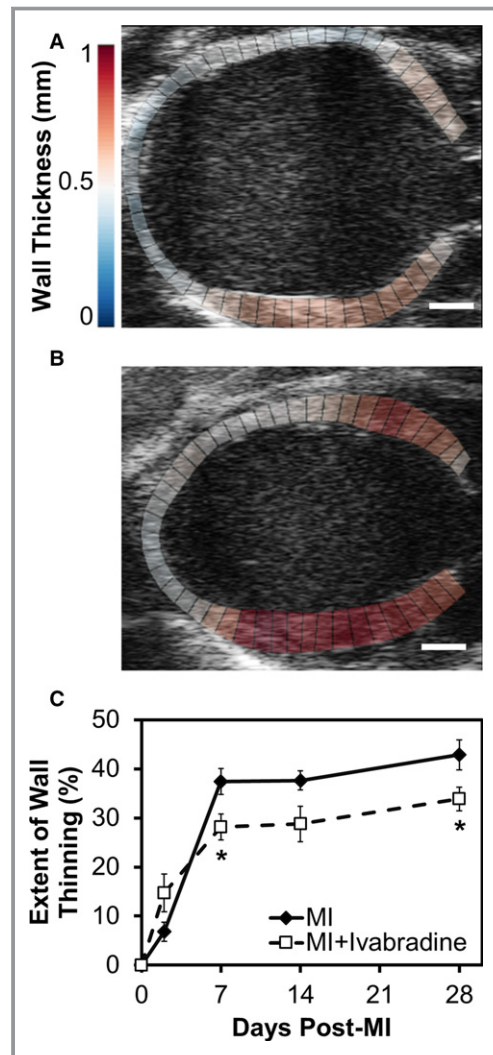


Figure 4. Ivabradine administration reduces the extent of wall thinning after MI. Representative long-axis ultrasound images of control (A) and ivabradine-treated mice (B) at end-diastole on day 28 post-MI are shown. Note that the chamber volume is appreciably smaller, and that the ventricular walls are appreciably thicker, in the ivabradine-treated heart (B), compared to the control heart (A). Scale bars=1 mm. C, The extent of wall thinning, measured as the percentage of long-axis tissue with a thickness of less than 0.5 mm, rapidly progressed after MI through day 7, and showed moderate progression from days 7 through 28 in both groups. The extent of wall thinning was reduced by 25% in ivabradine-treated mice (n=10) compared to infarcted controls (n=9) as early as day 7 post-MI and remained 21% smaller on day 28 (* $P < 0.05$). MI indicates myocardial infarction.

and control groups, respectively; $P < 0.05$). Regional analysis of the infarct zone revealed significant reductions of 56% and 54% in $E_{||}$ on day 2 post-MI in the control and ivabradine groups, respectively, compared to baseline ($P < 0.001$,

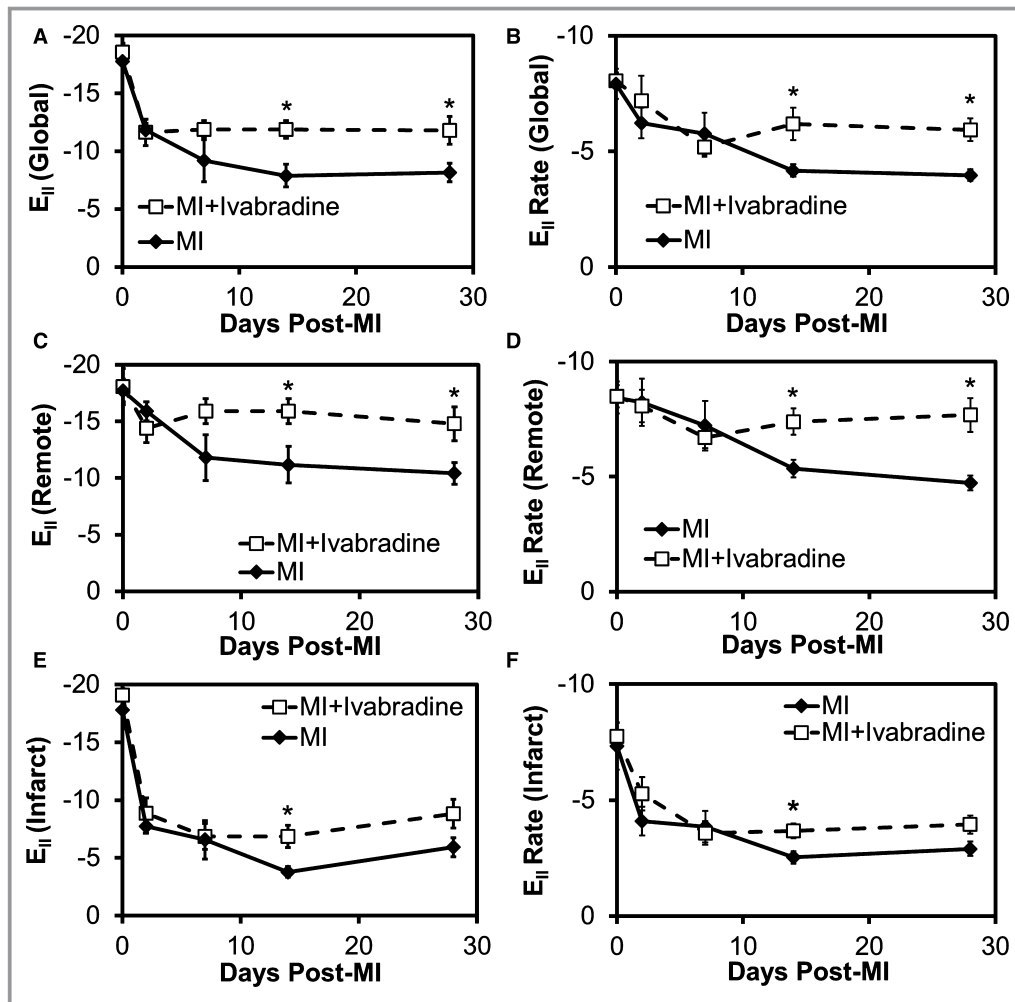


Figure 5. Ivabradine administration improves longitudinal strain and strain rate in noninfarcted myocardium. Speckle-tracking analysis of long-axis images at baseline and days 2, 7, 14, and 28 after MI was performed to determine the effects of ivabradine on regional and global peak longitudinal strain ($E_{||}$) and strain rate. A, Global analyses revealed an improvement in peak longitudinal strain on days 14 and 28, with a 44% higher $E_{||}$ in the ivabradine-treated group compared to the controls on day 28 post-MI. B, Global $E_{||}$ rate was also significantly improved in the ivabradine group on days 14 and 28. C, In the remote zone, ivabradine-treated animals were found to have significantly improved peak strain and (D) strain rate on days 14 and 28, compared with controls. The ivabradine-treated group showed modestly improved infarct zone (E) peak strain and (F) strain rate at later time points, although this improvement only achieved statistical significance on day 14. * $P < 0.05$ vs infarcted control group at the same time point. Data points in (A through F) represent mean \pm SEM of $n = 9$ infarcted control mice and $n = 10$ infarcted ivabradine mice. MI indicates myocardial infarction.

Figure 5E), while strain was better preserved in the remote zone (displaying nonsignificant 10% and 20% reductions in the control and ivabradine groups, respectively, compared to baseline; Figure 5C). In the remote zone, ivabradine-treated animals were found to have 42% greater peak strain on both days 14 and 28, compared to controls (-14.8 and -8.8 in the ivabradine and control groups on day 28; $P < 0.05$). In contrast, the ivabradine-treated group showed modestly improved peak strain in the infarct zone, reaching significance only on day 14 with $E_{||}$ values of -6.9 and -3.8 in the ivabradine and control groups, respectively.

The longitudinal strain rate presented a similar trend. From baseline to day-2 post MI, global $E_{||}$ rate declined from -7.9 ± 0.7 to -6.2 ± 0.7 s^{-1} in controls and from -8.1 ± 0.4 to -7.2 ± 1.1 s^{-1} in the ivabradine-treated animals (reductions of 10.9% and 21.3% in the ivabradine and control groups, respectively; $P < 0.05$; Figure 5B). Global $E_{||}$ rate continued to decline through day 28 in the control group, but leveled off by day 7 in the ivabradine group, leading to significant improvements on days 14 and 28, with a 50% improvement by day 28 versus the control group ($E_{||}$ rates of -5.9 and -4.0 s^{-1} in the ivabradine and control groups, respectively). Regional

analysis of $E_{||}$ rate in the infarct zone revealed drops of 32% in the ivabradine-treated group and 44% in the control group by day 2 post-MI compared to baseline (both $P < 0.05$ versus baseline; Figure 5F). Modest and nonsignificant decreases in day 2 strain rate compared to baseline (5% and 2%) were seen in the remote zone of the ivabradine and control groups, respectively (Figure 5D). At later time points, ivabradine-treated animals showed significant improvement in remote zone strain rate on days 14 and 28, with a 63% improvement in strain rate by day 28 compared to infarcted controls ($E_{||}$ rates of -7.7 and -4.7 s^{-1} in the ivabradine and control groups, respectively). Differences in the infarct zone at later time points were more modest, reaching significance only on day 14, with $E_{||}$ rates of -3.7 and -2.5 s^{-1} in the ivabradine and control groups, respectively.

Ivabradine Administration Reduces Post-MI LV Dyssynchrony

LV dyssynchrony was assessed at baseline and days 2, 7, 14, and 28 post-MI by analyzing intramural radial strain in the remote zone of the LV using short-axis images taken 1.5 to 2 mm from the cardiac base. Regional time-displacement curves in the 6-segment LV myocardium (Figure 6A) for representative examples of ivabradine-treated and control mice on day 28 are shown in Figure 6B and 6C, respectively. Note that the ivabradine-treated mouse demonstrates a greater magnitude and uniformity of time to peak displacement compared to the control mouse. These data were quantified using the standard deviation of time to peak radial strain ($SD T_{\text{Peak } E_{rr}}$) and TUS metrics (Figure 6F and 6G, respectively). $TUS^{29,31}$ is a ratio of the synchronous component of radial displacement to the sum of the synchronous and dyssynchronous components of radial displacement, following Fourier decomposition. Longitudinal evaluation of both TUS and $SD T_{\text{Peak } E_{rr}}$ after MI revealed dyssynchronous contraction among the LV myocardial segments developing over the time-course of LV remodeling in both groups, though this effect was less severe in ivabradine-treated mice. As a result, significant improvements in LV synchrony were observed on day 28 in ivabradine-treated mice, as measured by both metrics (a 29% decrease in $SD T_{\text{Peak}}$ and 16% increase in TUS; $P < 0.05$). Interestingly, a significant improvement in TUS was also observed at day 2 in ivabradine-treated versus control mice.

Discussion

In this study, ivabradine was shown to reduce heart rate in a mouse model of reperfused MI to a degree similar to previously studied animal models.^{15,17} We also believe this

to be the first report of mouse echocardiography performed after lateral thoracotomy via the third intercostal space. While this procedure is more technically challenging than the standard approach, we found a dramatic improvement in image quality with the incision site remote from the echocardiographic window. Using this surgical technique in combination with high-frequency ultrasound, the administration of ivabradine was shown to significantly reduce LV remodeling. Speckle-tracking-based strain analysis demonstrated improved longitudinal strain and strain rate in noninfarcted myocardium, indicating that heart rate reduction with ivabradine helps to preserve contractile function in the remote myocardium after MI. In addition, we demonstrated the ability of ivabradine to reduce dyssynchrony after MI.

These findings are consistent with a biomechanical model of LV remodeling, in which the progression of remodeling is proportional to heart rate. A reduction in heart rate decreases the total cumulative aberrant wall stress imposed on cardiomyocytes adjacent to the initial infarct,⁹ potentially decreasing infarct expansion. A decrease in heart rate also reduces oxygen demand and increases coronary diastolic perfusion time, thus potentially reducing ischemia in recovering myocardium.¹⁰ While this study did not directly examine the effects of ivabradine on myocardial metabolism, it is possible that this mechanism may also contribute to the attenuation of LV remodeling reported here. Reduced heart rate may also improve ventricular–arterial coupling and reduce afterload.³³ These mechanical effects are consistent with the findings of reduced wall thinning and decreased LV chamber volumes with ivabradine treatment compared to controls. Further evidence of reduced infarct expansion was manifested in greater loss of longitudinal strain and strain rate in the midanterior, apical-anterior, and apical-inferior wall segments of the heart (ie, the infarct zone) over the course of remodeling in the control group, even though late gadolinium-enhanced MRI indicated similar infarct size between groups on day 2 post-MI.

Ivabradine-treated mice also showed improved systolic functional parameters compared to the controls, including EF and remote-zone longitudinal strain and strain rate. Importantly, peak strain provides a measure of myocardial function independent of cardiac synchrony, unlike traditional functional parameters such as EF.³⁴ Global longitudinal strain has also been shown to be a superior predictor of all-cause mortality compared with EF.²⁵ Furthermore, strain rate has been shown to measure cardiac contractility relatively independent of changes in cardiac load and structure.³⁵

There are several intrinsic limitations to the accuracy of strain measurement using 2-dimensional echocardiographic speckle-tracking.³⁶ Given the helical arrangement of cardiac muscle fibers, some speckle in a 2-dimensional cine will move out of plane during each heartbeat, regardless of transducer

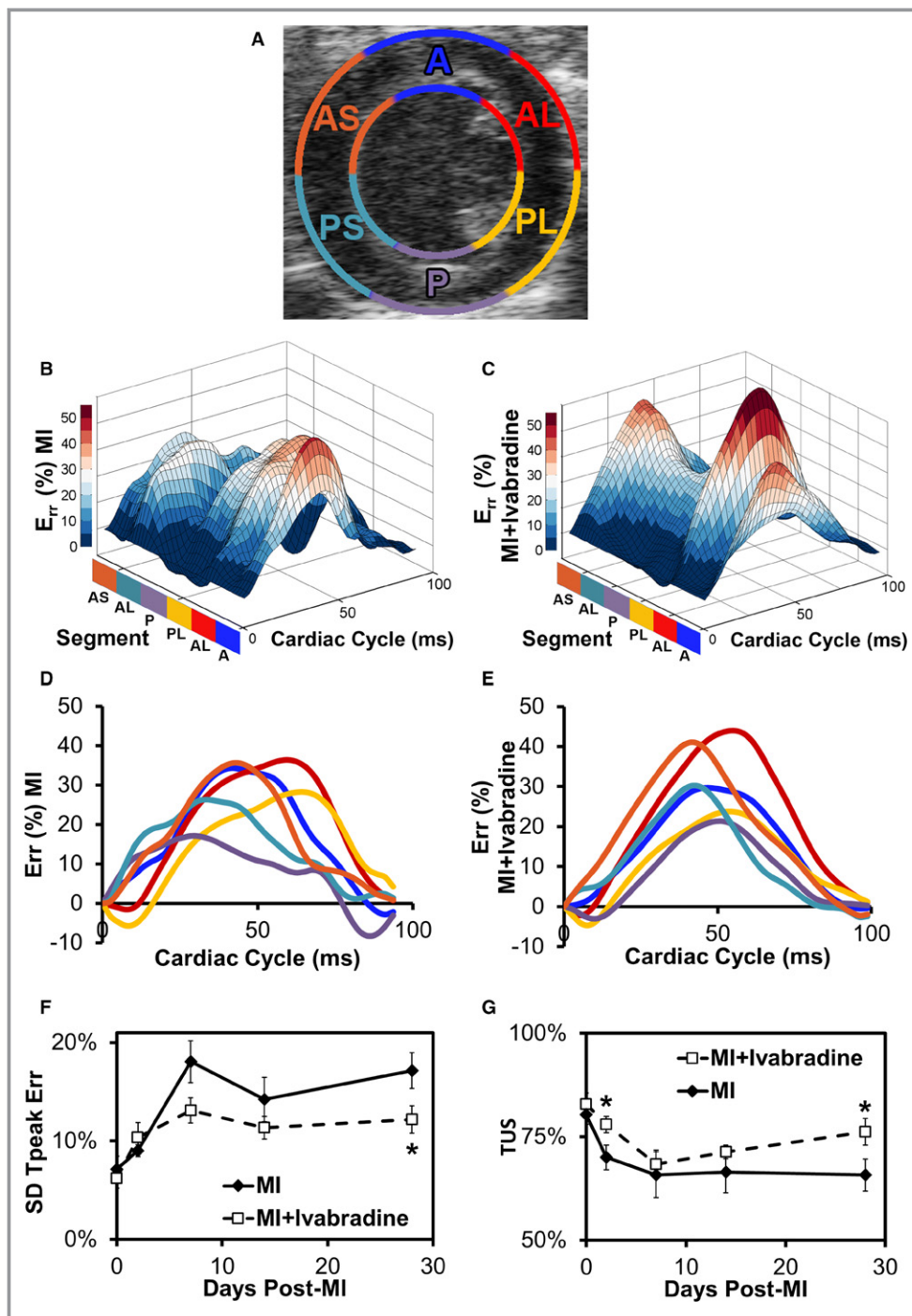


Figure 6. Ivabradine administration reduces post-MI LV dyssynchrony. A, Standard 6-sector LV short-axis segmentations are overlaid on a B-mode echocardiograph image taken 2 mm superior to the apex where dyssynchrony data were collected. A, anterior; AL, anterolateral; AS, anterior septum; P, posterior; PL, posterolateral; PS, posterior septum. B, Three-dimensional representation of SA endocardial radial strain over the course of a complete heart cycle at day 28 post-MI in a representative infarcted control and (C) an ivabradine-treated mouse. D, Time vs strain curves for each of the 6 sectors in a representative infarcted control and (E) an ivabradine-treated mouse. F, The standard deviation time to peak strain ($SD T_{peak}$) was significantly smaller in the ivabradine-treated group by day 28. G, Temporal uniformity of strain (TUS) was significantly greater in the ivabradine-treated group on days 2 and 28 post-MI, indicating more synchronous contraction. * $P < 0.05$ vs infarcted control group at the same time point. Data points in (F and G) represent mean \pm SEM of $n = 9$ infarcted control mice and $n = 10$ infarcted ivabradine mice. Err indicates radial strain; LV, left ventricular; MI, myocardial infarction; SA, short axis.

orientation. While this issue could be solved by employing 3-dimensional speckle tracking, current 3-dimensional transducers have neither the spatial nor temporal resolution necessary for murine imaging. Secondly, because speckle patterns are the product of ultrasound waves interacting with living tissue, they can vary slightly from one position to another in the heart. However, this inherent variability in speckle is minor compared to the ultrasound artifacts that can obscure or distort speckle patterns, thus diminishing tracking accuracy. In the current study, reproducibility was enhanced through the use of a highly standardized image acquisition protocol that included a bi-axial, micrometer-adjustable motion stage, a transducer controlled by an automated stepper motor for precise scan positioning, excluding mice with suboptimal baseline scans prior to randomization, and a novel surgical technique to reduce reverberation artifacts.

The finding of decreased dyssynchrony in ivabradine-treated mice may also coincide with current biomechanical models. Recent studies suggest that post-MI dyssynchrony may be linked to escalating mechanical dysfunction resulting from the changes in myocardial geometry and composition during the LV remodeling process, leading to a positive feedback between LV remodeling and cardiac dysfunction.^{11,37} Not surprisingly, the finding is also consistent with recent findings demonstrating that remote zone LV dyssynchrony develops in concert with global LV remodeling.¹¹ The finding that TUS was significantly reduced on day 2 in the ivabradine group may suggest a reduction in early systolic dyskinesia, at the time point when the myocardium is at its greatest risk of rupture.¹¹

While this study focused on *in vivo*, functional parameters of cardiac remodeling, previous studies have demonstrated reduced interstitial and periarteriolar collagen density,^{13,17} as well as improved cardiac calcium handling^{15,16} and preserved energy metabolism¹⁴ in ivabradine-treated animals after MI. These studies have also shown post-MI ivabradine treatment to attenuate increases in LV end-diastolic pressure¹⁷ and reduce markers of neuroendocrine activation.¹⁴ These effects are likely a combination of the direct effects of ivabradine treatment as well as downstream effects of improved remodeling.

While the biomechanical model presented here supports the role of heart rate reduction in attenuating LV remodeling, it does not rule out the potential pleiotropic effects of ivabradine treatment beyond pure heart rate reduction. Such effects were first observed by Heusch and colleagues, who showed that the ability of ivabradine to reduce acute infarct size was only partially attenuated by atrial pacing in a pig model of reperfused MI.³⁸ Because this finding was observed not only when ivabradine was given before the onset of ischemia, but also when given prior to reperfusion, it was hypothesized that ivabradine may have antioxidant effects. This was recently supported when Kleinbongard et al tested

the effects of ivabradine treatment on simulated ischemia/reperfusion in isolated murine cardiomyocytes.³⁹ They found that ivabradine treatment improved cardiomyocyte viability, reduced the accumulation of intra- and extracellular reactive oxygen species, and increased mitochondrial ATP production compared with untreated controls.

Decreased reactive oxygen species formation by ivabradine has also been demonstrated in the vascular tissue of apolipoprotein E knockout mice through NADPH oxidase inhibition⁴⁰ and the prevention of endothelial nitric oxide synthase uncoupling.⁴¹ Ivabradine treatment in vascular tissue was also shown to increase the expression of telomere-stabilizing proteins, indicating decreased cellular senescence.⁴¹ However, unlike in the isolated cardiomyocytes, these effects were absent in aortic rings treated *ex vivo*, in cultured vascular cells, and *in vivo* at a dose that did not lower heart rate. Given these findings, along with the fact that HCN channels are not expressed in vascular tissue, the beneficial effects of ivabradine were hypothesized to be the direct result of reduced shear stress at a reduced heart rate, rather than pleiotropic effects.⁴²

Recently, Gent and colleagues showed that mice given lifetime ivabradine treatment had a significantly longer lifespan than untreated mice, though they could not determine whether the longevity was secondary to heart rate reduction or to potential pleiotropic effects of ivabradine.⁴³ The authors hypothesized that reduced reactive oxygen species formation, either because of heart rate reduction or a direct action of ivabradine, would be mechanistically consistent with greater longevity, particularly as mice die mostly from cancer and not from cardiovascular disease, where the benefit from heart rate reduction would be more direct.

It has been suggested that pleiotropic effects of ivabradine may have also played a role in the results of the BEAUTIFUL study. A retrospective subgroup analysis demonstrated that the benefit of ivabradine treatment in terms of reduced mortality and hospitalization for acute MI in patients with anginal symptoms, LV dysfunction, and heart rate greater than 70 bpm was much larger than to be expected from a modest (at most 7 bpm) placebo-corrected heart rate reduction alone.^{44,45} In SHIFT, however, the benefit from ivabradine correlated with the magnitude of HR reduction.^{4,46} In order to elucidate the effects of ivabradine on LV remodeling beyond pure heart rate reduction, a remodeling study could be performed in paced ivabradine-treated animals.⁴⁷

It is informative to consider the results of the current study in the context of the recent large clinical trials studying ivabradine. SIGNIFY, which studied patients with stable coronary artery disease and without LV dysfunction, showed that patients treated with ivabradine did not have improved outcomes in terms of mortality from cardiovascular causes and myocardial infarction.⁴⁸ In patients with significant

angina, ivabradine even increased cardiovascular mortality and nonfatal myocardial infarction. This is in contrast to the BEAUTIFUL trial, which demonstrated reduced hospital admission for MI and reduced need for coronary revascularization in patients with chronic coronary artery disease and LV dysfunction and the SHIFT study, which showed a lower risk of death and hospitalization in patients with heart failure. Thus, while elevated heart rate is an independent *risk factor* in patients with LV dysfunction, in patients with normal LV function, elevated heart rate may instead only be a *risk marker* of other underlying processes that influence the development of MI (eg, diabetes and smoking).⁴⁹ This is in agreement with the biomechanical model presented here, in which heart rate reduction directly minimizes the aberrant pathophysiology imposed by the response to LV dysfunction secondary to myocardial infarction.

Importantly, the effects of ivabradine treatment in our study appear to have both acute and chronic components. Mice on ivabradine for 28 days showed greater EF and smaller ESV compared with mice acutely administered the drug from post-MI day 28 to 30. Furthermore, animals treated with ivabradine over 28 days and then taken off the drug showed lower heart rates and improved EF compared to mice never treated with the drug. While acute administration of the drug on days 28 to 30 lowered heart rate in previously untreated animals, no significant changes in EF or ESV were observed. This lack of improvement may be attributable to the low statistical power of the crossover study or may reflect the inability of the previously untreated mice to compensate for the reduced heart rate due to severe heart failure secondary to advanced LV remodeling.

This study reinforces the link between heart rate and LV remodeling after MI. Current guidelines for the management of patients with ST-elevation MI indicate β -blockers, which are negative chronotropes and inotropes, for use immediately after MI and during early recovery. However, heart rate often remains elevated in patients treated with β -blockers.⁵⁰ While the therapeutic benefit of ivabradine in combination with conventional therapies in the post-MI setting has yet to be determined, this study supports the need for more thorough investigation.

Acknowledgments

The authors wish to thank Arjun Dayal for his assistance designing software for the ultrasound image acquisition system.

Sources of Funding

This work was supported in part by NIH R01 HL092305 and R01 HL115225 to French and NIH R01 EB001826 to Hossack. The purchase of the VisualSonics Vevo2100

ultrasound instrument was funded with NIH S10 RR027333 to Hossack. The purchase of the Bruker ClinScan 7T MRI instrument was funded with NIH S10 RR019911 to Dr Stuart S. Berr.

Disclosures

None.

References

- Postea O, Biel M. Exploring HCN channels as novel drug targets. *Nat Rev Drug Discov*. 2011;10:903–914.
- Bucchi A, Baruscotti M, DiFrancesco D. Current-dependent block of rabbit sino-atrial node If channels by ivabradine. *J Gen Physiol*. 2002;120:1–13.
- Fox K, Ford I, Steg PG, Tendera M, Ferrari R. Ivabradine for patients with stable coronary artery disease and left-ventricular systolic dysfunction (BEAUTIFUL): a randomised, double-blind, placebo-controlled trial. *Lancet*. 2008;372:807–816.
- Swedberg K, Komajda M, Böhm M, Borer JS, Ford I, Dubost-Brama A, Lerebours G, Tavazzi L. Ivabradine and outcomes in chronic heart failure (SHIFT): a randomised placebo-controlled study. *Lancet*. 2010;376:875–885.
- Cecconi C, Freedman SB, Tardif JC, Hildebrandt P, McDonagh T, Gueret P, Parrinello G, Robertson M, Steg PG, Tendera M, Ford I, Fox K, Ferrari R. Effect of heart rate reduction by ivabradine on left ventricular remodeling in the echocardiographic substudy of BEAUTIFUL. *Int J Cardiol*. 2011;146:408–414.
- Tardif JC, O'Meara E, Komajda M, Böhm M, Borer JS, Ford I, Tavazzi L, Swedberg K. Effects of selective heart rate reduction with ivabradine on left ventricular remodelling and function: results from the SHIFT echocardiography substudy. *Eur Heart J*. 2011;32:2507–2515.
- McMurray JJV, Adamopoulos S, Anker SD, Auricchio A, Böhm M, Dickstein K, Falk V, Filippatos G, Fonseca C, Gomez-Sanchez MA. ESC guidelines for the diagnosis and treatment of acute and chronic heart failure 2012: the Task Force for the Diagnosis and Treatment of Acute and Chronic Heart Failure 2012 of the European Society of Cardiology. Developed in collaboration with the Heart Failure Association (HFA) of the ESC. *Eur Heart J*. 2012;33:1787–1847.
- Fosbøl EL, Seibæk M, Brendorp B, Møller DV, Thune JJ, Gislason GH, Torp-Pedersen C, Køber L. Long-term prognostic importance of resting heart rate in patients with left ventricular dysfunction in connection with either heart failure or myocardial infarction: the DIAMOND study. *Int J Cardiol*. 2010;140:279–286.
- French BA, Kramer CM. Mechanisms of postinfarct left ventricular remodeling. *Drug Discov Today Dis Mech*. 2007;4:185–196.
- Colin P, Ghaleh B, Monnet X, Hittinger L, Berdeaux A. Effect of graded heart rate reduction with ivabradine on myocardial oxygen consumption and diastolic time in exercising dogs. *J Pharmacol Exp Ther*. 2004;308:236–240.
- Li Y, Garson CD, Xu Y, Helm PA, Hossack JA, French BA. Serial ultrasound evaluation of intramyocardial strain after reperused myocardial infarction reveals that remote zone dyssynchrony develops in concert with left ventricular remodeling. *Ultrasound Med Biol*. 2011;37:1073–1086.
- O'Connor DM, Naresh NK, Piras BA, Xu Y, Smith RS, Epstein FH, Hossack JA, Ogle RC, French BA. A novel cardiac muscle-derived biomaterial reduces dyskinesia and postinfarct left ventricular remodeling in a mouse model of myocardial infarction. *Physiol Rep*. 2015;3:e12351.
- Christensen LP, Zhang R-L, Zheng W, Campanelli JJ, Dedkov EI, Weiss RM, Tomanek RJ. Postmyocardial infarction remodeling and coronary reserve: effects of ivabradine and beta blockade therapy. *Am J Physiol Heart Circ Physiol*. 2009;297:H322–H330.
- Cecconi C, Comini L, Suffredini S, Stilitano F, Bouly M, Cerbai E, Mugelli A, Ferrari R. Heart rate reduction with ivabradine prevents the global phenotype of left ventricular remodeling. *Am J Physiol Heart Circ Physiol*. 2011;300:H366–H373.
- Couvreur N, Tissier R, Pons S, Chetboul V, Gouni V, Bruneval P, Mandet C, Pouchelon J-L, Berdeaux A, Ghaleh B. Chronic heart rate reduction with ivabradine improves systolic function of the reperfused heart through a dual mechanism involving a direct mechanical effect and a long-term increase in FKBP12/12.6 expression. *Eur Heart J*. 2010;31:1529–1537.
- Maczewski M, Mackiewicz U. Effect of metoprolol and ivabradine on left ventricular remodelling and Ca²⁺ handling in the post-infarction rat heart. *Cardiovasc Res*. 2008;79:42–51.
- Dedkov EI, Zheng W, Christensen LP, Weiss RM, Mahlberg-Gaudin F, Tomanek RJ. Preservation of coronary reserve by ivabradine-induced reduction in heart

- rate in infarcted rats is associated with decrease in perivascular collagen. *Am J Physiol Heart Circ Physiol*. 2007;293:H590–H598.
18. Steg P, Lopez-de-Sà E, Schiele F, Hamon M, Meinertz T, Goicolea J, Werdan K, Lopez-Sendon J. Safety of intravenous ivabradine in acute ST-segment elevation myocardial infarction patients treated with primary percutaneous coronary intervention: a randomized, placebo-controlled, double-blind, pilot study. *Eur Heart J Acute Cardiovasc Care*. 2013;2:270–279.
 19. Gerbaud E, Montaudon M, Chasseriaud W, Gilbert S, Cochet H, Pucheu Y, Horovitz A, Bonnet J, Douard H, Coste P. Effect of ivabradine on left ventricular remodelling after reperfusion myocardial infarction: a pilot study. *Arch Cardiovasc Dis*. 2014;107:33–41.
 20. Du X-J, Feng X, Gao X-M, Tan TP, Kiriazis H, Dart AM. If channel inhibitor ivabradine lowers heart rate in mice with enhanced sympathoadrenergic activities. *Br J Pharmacol*. 2004;142:107–112.
 21. Helm PA, Caravan P, French BA, Jacques V, Shen L, Xu Y, Beyers RJ, Roy RJ, Kramer CM, Epstein FH. Postinfarction myocardial scarring in mice: molecular MR imaging with use of a collagen-targeting contrast agent. *Radiology*. 2008;247:788–796.
 22. Gilson WD, Epstein FH, Yang Z, Xu Y, Prasad K-MR, Toufektsian M-C, Laubach VE, French BA. Borderzone contractile dysfunction is transiently attenuated and left ventricular structural remodeling is markedly reduced following reperfusion myocardial infarction in inducible nitric oxide synthase knockout mice. *J Am Coll Cardiol*. 2007;50:1799–1807.
 23. Bauer M, Cheng S, Jain M, Ngoy S, Theodoropoulos C, Trujillo A, Lin F-C, Liao R. Echocardiographic speckle-tracking based strain imaging for rapid cardiovascular phenotyping in mice. *Circ Res*. 2011;108:908–916.
 24. Manovel A, Dawson D, Smith B, Nihoyannopoulos P. Assessment of left ventricular function by different speckle-tracking software. *Eur J Echocardiogr*. 2010;11:417–421.
 25. Stanton T, Leano R, Marwick TH. Prediction of all-cause mortality from global longitudinal speckle strain: comparison with ejection fraction and wall motion scoring. *Circ Cardiovasc Imaging*. 2009;2:356–364.
 26. Cerqueira MD, Weissman NJ, Dilsizian V, Jacobs AK, Kaul S, Laskey WK, Pennell DJ, Rumberger JA, Ryan T, Verani MS; American Heart Association Writing Group on Myocardial Segmentation and Registration for Cardiac Imaging. Standardized myocardial segmentation and nomenclature for tomographic imaging of the heart. A statement for healthcare professionals from the Cardiac Imaging Committee of the Council on Clinical Cardiology of the American Heart Association. *Circulation*. 2002;105:539–542.
 27. Li Y, Garson CD, Xu Y, French BA, Hossack JA. High frequency ultrasound imaging detects cardiac dyssynchrony in noninfarcted regions of the murine left ventricle late after reperfusion myocardial infarction. *Ultrasound Med Biol*. 2008;34:1063–1075.
 28. Tanabe M, Lamia B, Tanaka H, Schwartzman D, Pinsky MR, Gorcsan J. Echocardiographic speckle tracking radial strain imaging to assess ventricular dyssynchrony in a pacing model of resynchronization therapy. *J Am Soc Echocardiogr*. 2008;21:1382–1388.
 29. Helm RH, Leclercq C, Faris OP, Ozturk C, McVeigh E, Lardo AC, Kass DA. Cardiac dyssynchrony analysis using circumferential versus longitudinal strain implications for assessing cardiac resynchronization. *Circulation*. 2005;111:2760–2767.
 30. Delgado V, Ypenburg C, van Bommel RJ, Tops LF, Mollema SA, Marsan NA, Bleeker GB, Schalij MJ, Bax JJ. Assessment of left ventricular dyssynchrony by speckle tracking strain imaging comparison between longitudinal, circumferential, and radial strain in cardiac resynchronization therapy. *J Am Coll Cardiol*. 2008;51:1944–1952.
 31. Leclercq C, Faris O, Tunin R, Johnson J, Kato R, Evans F, Spinelli J, Halperin H, McVeigh E, Kass DA. Systolic improvement and mechanical resynchronization does not require electrical synchrony in the dilated failing heart with left bundle-branch block. *Circulation*. 2002;106:1760–1763.
 32. Ross AJ, Yang Z, Berr SS, Gilson WD, Petersen WC, Oshinski JN, French BA. Serial MRI evaluation of cardiac structure and function in mice after reperfusion myocardial infarction. *Magn Reson Med*. 2002;47:1158–1168.
 33. Reil J-C, Tardif J-C, Ford I, Lloyd SM, O'Meara E, Komajda M, Borer JS, Tavazzi L, Swedberg K, Böhm M. Selective heart rate reduction with ivabradine unloads the left ventricle in heart failure patients. *J Am Coll Cardiol*. 2013;62:1977–1985.
 34. Blyakhman FA, Naidich AM, Kolchanova SG, Sokolov SY, Kremleva YV, Chestukhin VV. Validity of ejection fraction as a measure of myocardial functional state: impact of asynchrony. *Eur J Echocardiogr*. 2009;10:613–618.
 35. Ferferieva V, Van den Bergh A, Claus P, Jasaityte R, Veulemans P, Pellens M, La Gerche A, Rademakers F, Herijgers P, D'hooge J. The relative value of strain and strain rate for defining intrinsic myocardial function. *Am J Physiol Heart Circ Physiol*. 2012;302:H188–H195.
 36. Voigt J-U, Pedrizzetti G, Lysyansky P, Marwick TH, Houle H, Baumann R, Pedri S, Ito Y, Abe Y, Metz S, Song JH, Hamilton J, Sengupta PP, Kolias TJ, d'Hooge J, Aurigemma GP, Thomas JD, Badano LP. Definitions for a common standard for 2D speckle tracking echocardiography: consensus document of the EACVI/ASE/Industry Task Force to standardize deformation imaging. *Eur Heart J Cardiovasc Imaging*. 2015;16:1–11.
 37. Mann DL, Bristow MR. Mechanisms and models in heart failure: the biomechanical model and beyond. *Circulation*. 2005;111:2837–2849.
 38. Heusch G, Skyschally A, Gres P, van Caster P, Schilawa D, Schulz R. Improvement of regional myocardial blood flow and function and reduction of infarct size with ivabradine: protection beyond heart rate reduction. *Eur Heart J*. 2008;29:2265–2275.
 39. Kleinbongard P, Gedik N, Witting P, Freedman B, Klöcker N, Heusch G. Pleiotropic, heart rate-independent cardioprotection by ivabradine. *Br J Pharmacol*. 2015;172:4380–4390.
 40. Custodis F, Baumhäkel M, Schlimmer N, List F, Gensch C, Böhm M, Laufs U. Heart rate reduction by ivabradine reduces oxidative stress, improves endothelial function, and prevents atherosclerosis in apolipoprotein E-deficient mice. *Circulation*. 2008;117:2377–2387.
 41. Kröller-Schön S, Schulz E, Wenzel P, Kleschyov AL, Hortmann M, Torzewski M, Oelze M, Renné T, Daiber A, Münzel T. Differential effects of heart rate reduction with ivabradine in two models of endothelial dysfunction and oxidative stress. *Basic Res Cardiol*. 2011;106:1147–1158.
 42. Heusch G. Pleiotropic action(s) of the bradycardic agent ivabradine: cardiovascular protection beyond heart rate reduction. *Br J Pharmacol*. 2008;155:970–971.
 43. Gent S, Kleinbongard P, Dammann P, Neuhäuser M, Heusch G. Heart rate reduction and longevity in mice. *Basic Res Cardiol*. 2015;110:1–9.
 44. Fox K, Ford I, Steg PG, Tendera M, Robertson M, Ferrari R. Relationship between ivabradine treatment and cardiovascular outcomes in patients with stable coronary artery disease and left ventricular systolic dysfunction with limiting angina: a subgroup analysis of the randomized, controlled BEAUTIFUL trial. *Eur Heart J*. 2009;30:2337–2345.
 45. Heusch G. A BEAUTIFUL lesson—ivabradine protects from ischaemia, but not from heart failure: through heart rate reduction or more? *Eur Heart J*. 2009;30:2300–2301.
 46. Heusch G. Heart rate and heart failure. *Circ J*. 2011;75:229–236.
 47. Heusch G, Skyschally A, Schulz R. Cardioprotection by ivabradine through heart rate reduction and beyond. *J Cardiovasc Pharmacol Ther*. 2011;16:281–284.
 48. Fox K, Ford I, Steg PG, Tardif J-C, Tendera M, Ferrari R. Ivabradine in stable coronary artery disease without clinical heart failure. *N Engl J Med*. 2014;371:1091–1099.
 49. Ferrari R, Fox KM. The role of heart rate may differ according to pathophysiological setting: from SHIFT to SIGNIFY. *Eur Heart J*. 2015;36:2042–2046.
 50. Komajda M, Follath F, Swedberg K, Cleland J, Aguilar JC, Cohen-Solal A, Dietz R, Gavazzi A, Gilst WHV, Hobbs R, Korewicki J, Madeira HC, Moiseyev VS, Preda I, Widimsky J, Freemantle N, Eastaugh J, Mason J. The EuroHeart Failure Survey programme—a survey on the quality of care among patients with heart failure in Europe Part 2: treatment. *Eur Heart J*. 2003;24:464–474.